

# A Conductance Study of Guanidinium Chloride, Thiocyanate, Sulfate, and Carbonate in Dilute Aqueous Solutions: Ion-Association and Carbonate Hydrolysis Effects

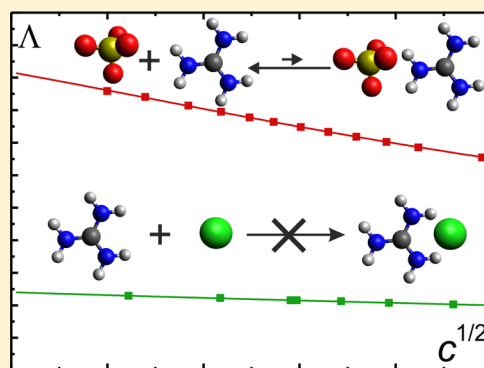
Johannes Hunger,<sup>\*,†,‡</sup> Roland Neueder,<sup>†</sup> Richard Buchner,<sup>†</sup> and Alexander Apelblat<sup>§</sup>

<sup>†</sup>Institut für Physikalische und Theoretische Chemie, Universität Regensburg, 93040 Regensburg, Germany

<sup>‡</sup>Max Planck Institute for Polymer Research, Ackermannweg 10, 55128 Mainz, Germany

<sup>§</sup>Department of Chemical Engineering, Ben-Gurion University of the Negev, 84105 Beer Sheva, Israel

**ABSTRACT:** We study the conductance of dilute aqueous solutions for a series of guanidinium salts at 298.15 K. The experimental molar conductivities were analyzed within the framework of the Quint–Viallard theory in combination with Debye–Hückel activity coefficients. From this analysis, we find no evidence for significant ion association in aqueous solutions of guanidinium chloride (GdmCl) and guanidinium thiocyanate (GdmSCN), and the molar conductivity of these electrolytes can be modeled assuming a complete dissociation. The limiting ionic conductivity of the guanidinium ion ( $\text{Gdm}^+$ ) is accurately determined to  $\lambda_{\text{Gdm}^+} = 51.45 \pm 0.10 \text{ S cm}^2 \text{ mol}^{-1}$ . For the bivalent salts guanidinium sulfate ( $\text{Gdm}_2\text{SO}_4$ ) and guanidinium carbonate ( $\text{Gdm}_2\text{CO}_3$ ), the molar conductivities show small deviations from ideal (fully dissociated electrolyte) behavior, which are related to weak ion association in solution. Furthermore, for solutions of  $\text{Gdm}_2\text{CO}_3$ , the hydrolysis of the carbonate anion leads to distinctively increased molar conductivities at high dilutions. The observed ion association is rather weak for all studied electrolytes and cannot explain the different protein denaturing activities of the studied guanidinium salts, as has been proposed previously.



## INTRODUCTION

Guanidinium thiocyanate ( $\text{GdmSCN}$ ,  $\text{C}(\text{NH}_2)_3\text{SCN}$ ) and guanidinium chloride ( $\text{GdmCl}$ ) are among the most powerful protein denaturants. They are commonly used to efficiently convert proteins from their native state into random coils,<sup>1</sup> and this denaturing activity is occasionally associated with specific properties of the guanidinium cation.<sup>2,3</sup> However, it has been shown as early as in 1965 that, for a series of  $\text{Gdm}^+$  salts, the Hofmeister series is obeyed<sup>4</sup> and the protein denaturing activity shows a distinct dependence on the counterion. For a series of guanidinium salts, a strong protein denaturing activity was observed for the thiocyanate, chloride, and acetate salt of guanidinium, while the sulfate salt of  $\text{Gdm}^+$  tends to stabilize proteins.<sup>4,5</sup>

Thus, the action of electrolytes toward biomolecules cannot be explained by the specific property of an individual ion. Instead, the entire solution structure and energetics need to be taken into account. Due to the long-ranging Coulomb forces present in electrolyte solutions, such systems deviate significantly from (thermodynamically) ideal behavior already at low solute concentrations and their structural properties may be rather complex. One important aspect of the structure of electrolytes is that Coulomb attraction can lead to the association of oppositely charged ions in solution, which alters the macroscopic solution properties.<sup>6,7</sup> Such ion aggregates play an important role as the initial nuclei during crystallization<sup>8</sup> and are relevant in living organisms.<sup>9,10</sup>

Recently, molecular dynamics simulations have suggested<sup>11–15</sup> that ion association may explain the difference in activity toward proteins for different guanidinium salts. These studies found moderate ion association in aqueous solution of  $\text{GdmSCN}$ <sup>11</sup> and  $\text{GdmCl}$ ,<sup>12,16</sup> while for aqueous solutions of  $\text{Gdm}_2\text{CO}_3$ <sup>13</sup> and  $\text{Gdm}_2\text{SO}_4$ <sup>14</sup> unexpectedly pronounced heteroion pairing was observed. Some simulations<sup>13,14</sup> even suggest that these ion aggregates extended to nanometer sized aggregates for bivalent guanidinium salts. Such aggregates drastically reduce the activity of the guanidinium ion in solution, and it has been suggested<sup>13,14</sup> that the absence of a denaturing activity can be traced back to this lowered activity of the  $\text{Gdm}^+$  ion in solutions of  $\text{Gdm}_2\text{CO}_3$  and  $\text{Gdm}_2\text{SO}_4$ . However, the formation of these ion aggregates is still controversially discussed,<sup>17–19</sup> and it has been shown recently that the degree of aggregation obtained from molecular dynamics simulation depends significantly on the force fields used.<sup>20–22</sup> Furthermore, no evidence for the proposed ion aggregates has been found with dielectric relaxation spectroscopy for  $\text{GdmCl}$  and  $\text{Gdm}_2\text{CO}_3$ .<sup>19</sup>

Accurate speciation of ion aggregation in solution remains a challenge, as many experimental techniques require high salt concentrations to yield detectable effects.<sup>6</sup> However, at high

Received: September 26, 2012

Published: December 13, 2012

solute concentrations, steric crowding and random collisions may lead to regular ion contacts, but due to their statistical nature, such short-lived ion contacts provide no direct information on the strength of specific ion–ion interactions. Even more, due to the short interionic distances in such concentrated systems, the increased ion pair–ion interactions often lead to a breakup of the aggregates, the well-known redissociation effect,<sup>23</sup> so that “true” ion pairs (i.e., species with a lifetime exceeding diffusion-controlled decay) disappear despite increasing direct ion–ion contacts. A direct measure for the strength of solute–solute interactions in solution is the (thermodynamic) standard association constant,  $K_A$ , at infinite dilution because here random solute–solute contacts are insignificant, so that  $K_A$  solely reflects the balance of solvation forces and specific anion–cation interactions.<sup>6,24,25</sup> For dilute electrolyte solutions, conductance studies are particularly suited to detect any kind of ion association and quantify the standard equilibrium constants.<sup>6,24,26–29</sup> For symmetric electrolytes (e.g., 1:1 electrolyte), ions bound in stable ion pairs do not contribute to the macroscopic conductivity due to their zero net charge. Also, for asymmetric electrolytes (e.g., 2:1 electrolytes), ion aggregates reduce the number of charge carriers in solution and the associated ions possess a lower mobility due to the increased hydrodynamic volume. For both cases, ion pairing leads to a marked reduction of the conductance compared to the limiting case of a completely dissociated electrolyte solution. This fact renders conductance measurements an excellent tool to study the association behavior of salt solutions.

We report on a detailed conductance study of dilute aqueous solutions ( $c < 28 \text{ mol m}^{-3}$ ) of GdmCl, GdmSCN, Gdm<sub>2</sub>SO<sub>4</sub>, and Gdm<sub>2</sub>CO<sub>3</sub> at 298.15 K. The experimental conductivities were analyzed within the framework of the Quint–Viallard theory<sup>30–32</sup> together with Debye–Hückel activity coefficients. We determine the degree of ion association for all studied salts, and we account for the hydrolysis of the carbonate ion for solution of Gdm<sub>2</sub>CO<sub>3</sub> in our model for the macroscopic conductance.

## EXPERIMENTAL SECTION

**Materials.** Guanidinium thiocyanate (>98%, Merck, Germany), guanidinium sulfate (>99%, Sigma-Aldrich, Germany), and guanidinium carbonate (>99%, Merck, Germany) were used without further purification. Samples of guanidinium chloride (GdmCl) were prepared by adding an ~20% molar excess of concentrated HCl (analytical grade, 36%, Fisher Scientific, U.K.) to an aqueous solution of Gdm<sub>2</sub>CO<sub>3</sub>. After evaporation of excess HCl and water, the raw product was recrystallized thrice from ethanol (analytical grade, >99.9%, J. T. Baker, Netherlands). All salts were dried under a vacuum ( $p < 10^{-8} \text{ bar}$ ) at ~350 K for 3 days and stored in a N<sub>2</sub>-filled glovebox. For the conductance measurements, guanidinium salt stock solutions were prepared using an analytical balance without buoyancy correction. Degassed Millipore MILLI-Q water with conductivities of  $\kappa < 5 \times 10^{-7} \text{ S cm}^{-1}$  was used for all samples.

**Conductivity Measurements.** Conductivity measurements were performed using a three-electrode flow cell connected to a mixing chamber described in detail elsewhere.<sup>33,34</sup> The cell is immersed in a temperature bath fed by a hydraulically sealed circulation thermostat (Unistat 705w, Peter Huber Kältemaschinenbau, Germany). To increase the temperature stability, the bath liquid (Silicon oil M5, Carl Roth, Germany) is pre-thermostated in a heat-exchange buffer unit enclosing the

temperature bath (Figure 1). Thus, a long-term (>5 h) temperature stability better than  $\pm 0.003 \text{ K}$  is achieved.

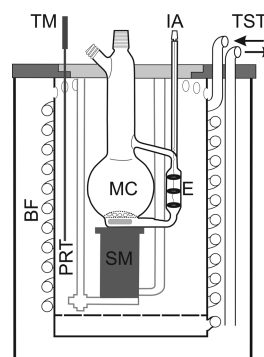


**Figure 1.** Schematic representation of the experimental setup with the measurement cell immersed in the temperature bath (TM, thermometer connection; IA, impedance analyzer connection; TST, circulation thermostat connection; MC, mixing chamber; E, electrode assembly; BF, pre-thermostating buffer; SM, stirrer motor; PRT, platinum resistance thermometer).

The temperature of the cell is measured with a (NIST-traceable) platinum resistance thermometer (PT-100), which is placed in the bath and connected to a high precision thermometer (F250a, Automatic Systems Laboratories, U.K.). The temperature measurement is accurate to  $\pm 0.01 \text{ K}$  with a precision of  $\pm 0.001 \text{ K}$ .

To determine the conductance of the sample, the impedance of the cell is measured using a LCR Bridge (HM8118, HAMEG Instruments GmbH, Germany) with a basic accuracy of 0.05% at frequencies,  $\nu$ , ranging from 100 Hz to 2 kHz. To account for electrode polarization effects, the real part of the impedance (i.e., the resistance,  $R$ ) is extrapolated to infinite frequencies yielding the resistance of the cell,  $R_\infty$ .<sup>35,36</sup> The specific conductance of the sample,  $\kappa = C/R_\infty$ , is obtained using the cell constant  $C$ , which was determined to  $C = 4.7565 \pm 0.0012 \text{ cm}^{-1}$  from calibration measurements using aqueous potassium chloride solutions.<sup>34</sup>

The measurement procedure is automated using Labview (National Instruments), and readings of temperature as well as a series of impedances as a function of frequency were taken at intervals of 90 s. Readings were averaged over a period of ~30 min once the temperature had equilibrated.

At the beginning of every measurement cycle, the cell was filled with a weighed amount of water (~680 g) under a nitrogen atmosphere. After the measurement of the solvent conductivity, weighed amounts of stock solution were added subsequently using a gastight buret. The measured specific conductivity at each concentration was converted to the molar conductivity,  $\Lambda = \kappa/c$ , where  $c$  is the solute concentration (in  $\text{mol L}^{-1}$ ).

**Density Measurements.** Solution densities,  $\rho$ , required for the calculation of molar concentrations,  $c$ , were interpolated from literature values where available (GdmCl, Gdm<sub>2</sub>CO<sub>3</sub>).<sup>19</sup> For samples of GdmSCN and Gdm<sub>2</sub>SO<sub>4</sub>, densities were determined using a vibrating tube densimeter (DMA 5000, Anton Paar GmbH, Austria) to an accuracy of  $5 \times 10^{-1} \text{ g dm}^{-3}$ . Densities were measured for selected compositions and were interpolated using a linear relation of the density as a function of weight fraction,  $w$  ( $\rho = 997.048 \text{ g dm}^{-3} + wB$ ).<sup>37</sup> The measured densities together with the slope of the linear regression,  $B$ , are listed in Table 1.

**Table 1.** Solute Mass Fractions,  $w$ , Together with Their Measured Densities,  $\rho$ , at 298.15 K<sup>a</sup>

GdmCl		Gdm <sub>2</sub> CO <sub>3</sub>	
$B = 281.89 \pm 0.59 \text{ g}^{-1} \text{ dm}^3 \text{ }^b$		$B = 431.66 \pm 1.54 \text{ g}^{-1} \text{ dm}^3 \text{ }^b$	
GdmSCN		Gdm <sub>2</sub> SO <sub>4</sub>	
$B = 234.72 \pm 0.31 \text{ g}^{-1} \text{ dm}^3$		$B = 460.15 \pm 1.36 \text{ g}^{-1} \text{ dm}^3$	
$w \cdot 10^5$	$\rho \text{ (g dm}^{-3}\text{)}$	$w \cdot 10^5$	$\rho \text{ (g dm}^{-3}\text{)}$
913.55	999.197	677.38	1000.211
1521.1	1000.630	1784.1	1005.277
2295.3	1002.426	2302.0	1007.612

<sup>a</sup> $B$  corresponds to the slope of the linear regression  $\rho = 997.048 \text{ g dm}^{-3} + wB$ . <sup>b</sup>Value obtained from measured densities reported in ref 19.

## ■ DATA ANALYSIS

**Conductivity Equations.** The measured molar conductances,  $\Lambda$ , are related to the properties of individual ions via

$$\Lambda = \frac{\kappa}{c} = \sum_{i=1}^n \frac{|z_i|c_i\lambda_i}{c} \quad (1)$$

where  $\lambda_i$  is the ionic conductivity,  $c_i$  the concentration, and  $z_i$  the valency of the individual ions,  $i = 1, \dots, n$ . The ionic conductivity exhibits a pronounced dependence on the concentration of all ions in solution, which is defined by the ionic strength  $I = \frac{1}{2} \sum_{i=1}^n c_i z_i^2$ . For dilute solutions of mixed electrolytes,  $\lambda_i(I)$  can be obtained within the framework of the Quint–Villard theory:<sup>30–32</sup>

$$\lambda_i = \lambda_i^\circ - S_i \sqrt{I} + E_i I \ln I + J_{1i} I - J_{2i} I^{3/2} \quad (2)$$

where  $\lambda_i^\circ$  is the limiting conductance at infinite dilution of ion  $i$ . The coefficients  $S_i$ ,  $E_i$ ,  $J_{1i}$ , and  $J_{2i}$  account for the electrophoretic effect and the ion cloud relaxation in solution. At a given temperature, they are a function of the solvent viscosity,  $\eta$ , dielectric permittivity,  $\epsilon$ , and all ionic conductivities at infinite dilution,  $\lambda_i^\circ$ . For the present study, the viscosity of water and its dielectric permittivity at 298.15 K were taken from the literature ( $\epsilon = 78.358$ ,<sup>38</sup>  $\eta = 0.8903 \text{ mPa s}^{39}$ ). The parameters

$J_{1i}$  and  $J_{2i}$  also depend on the distance of closest approach,  $R = 2(r_{S,-} + r_{S,+})$  with the hydrodynamic (Stokes) radii of the anion,  $r_{S,-}$ , and the cation,  $r_{S,+}$ . The analytical expressions for these parameters are rather complex<sup>30–32</sup> and can be found elsewhere.<sup>40–42</sup>

**Chemical Equilibria.** In electrolyte solutions, chemical reactions or association equilibria will alter the concentration and the ionic species that are present in solution. In particular, the association of ions resulting in the formation of ion pairs and the hydrolysis of the carbonate ion are relevant for the present work. According to the mass-action equation, such reactions are characterized by their corresponding equilibrium constants,  $K$ , the equilibrium concentrations,  $c_i$ , and the corresponding activity coefficients,  $f_i$ :

$$K = \prod_i (c_i f_i)^{\nu_i} \quad (3)$$

The exponents  $\nu_i$  in eq 3 are the stoichiometric coefficients in the corresponding chemical reaction. To determine the activity coefficients,  $f_i$ , of the individual ions in solution, the Debye–Hückel theory is used:

$$\log f_i = -\frac{z_i^2 A \sqrt{I}}{1 + 2r_{S,i} B \sqrt{I}} \quad (4)$$

In eq 4,  $A (=0.511 \text{ L}^{1/2} \text{ mol}^{-1/2})$  and  $B (=3.301 \times 10^9 \text{ L}^{1/2} \text{ mol}^{-1/2} \text{ m}^{-1})$  are the Debye–Hückel coefficients for water at 298.15 K and  $r_{S,i}$  is the hydrodynamic radius of the ion.

As any chemical equilibrium, being it an association or a reaction, will alter the ionic strength of the solution (due to the variation of the ionic species in solution), eqs 3 and 4 are dependent. This means that activity coefficients are affecting the equilibrium concentrations,  $c_i$ , in eq 3, which leads to a change in the ionic strength. In turn, this results in a change in the activity coefficients. Therefore, we use an iterative technique to obtain the equilibrium concentrations  $c_i$  in eq 3 for a given equilibrium constant  $K$ .

## ■ RESULTS

We measure the conductivities for aqueous solution of four different guanidinium salts at 298.15 K. We compare the

**Table 2.** Molar Concentrations,  $c$ , Measured Molar Conductivities,  $\Lambda_m$ , and Calculated Molar Conductivities,  $\Lambda_c$ , According to eqs 5 and 6 for Dilute Aqueous Solutions of GdmCl and GdmSCN, Respectively, at 298.15 K

GdmCl			GdmSCN		
$c \text{ (mol m}^{-3}\text{)}$	$\Lambda_m \text{ (S cm}^2 \text{ mol}^{-1}\text{)}$	$\Lambda_c \text{ (S cm}^2 \text{ mol}^{-1}\text{)}$	$c \text{ (mol m}^{-3}\text{)}$	$\Lambda_m \text{ (S cm}^2 \text{ mol}^{-1}\text{)}$	$\Lambda_c \text{ (S cm}^2 \text{ mol}^{-1}\text{)}$
0.59541	125.87	125.73	0.78176	115.73	115.41
1.8901	124.55	124.17	1.3001	114.94	114.77
3.3753	123.15	123.03	2.2177	114.26	113.92
3.5273	123.19	122.25	2.6499	113.83	113.60
4.7087	122.54	122.94	2.9388	113.70	113.40
6.1706	121.57	121.54	4.2061	112.96	112.63
8.4601	120.61	120.60	5.6687	112.09	111.91
11.860	119.32	119.48	6.6895	111.40	111.47
15.751	118.10	118.44	8.1783	110.79	110.90
27.073	115.40	116.15	8.6366	110.68	110.74
			10.454	110.14	110.16
			12.560	109.48	109.55
			15.581	108.61	108.79
			18.258	107.85	108.20
			21.058	107.23	107.64
			27.131	105.97	106.58

univalent GdmCl and GdmSCN salts (Table 2, Figure 2) to the bivalent sulfate and carbonate salts (Table 3, Figures 3 and 4)

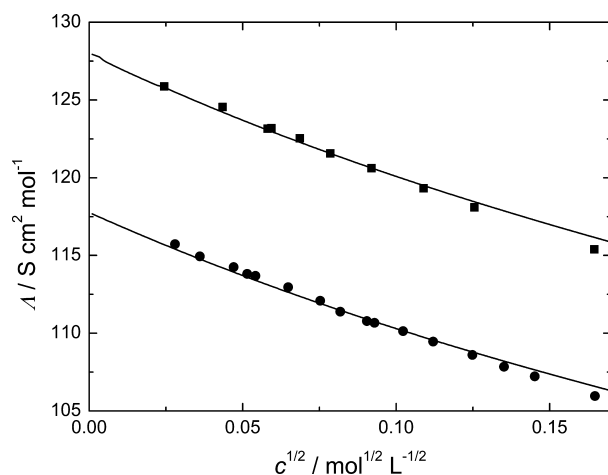


**Figure 2.** Molar conductivity,  $\Lambda$ , of aqueous solutions of GdmCl (■) and GdmSCN (●) at 298.15 K. Symbols correspond to experimental data, and lines show fits according to our model assuming fully dissociated electrolytes (see text).

of the guanidinium ion. As can be seen in Figures 2–4, the values for  $\Lambda(c)$  decrease with increasing concentration for all measured salts. This decrease stems from the reduced mobility of the ions due to the relaxation of the diffusive ion cloud and the electrophoretic counter current according to eq 2.

**Guanidinium Chloride.** The simplest systems of the present study are the univalent salts. As can be seen in Figure 2, the molar conductivities of GdmCl exhibit a nearly linear decrease as a function of the square root concentration. Such a  $\Lambda(c)$  decrease is commonly observed for weakly associated electrolytes, and we model the experimental conductivities assuming GdmCl to be fully dissociated in solution. Therefore,

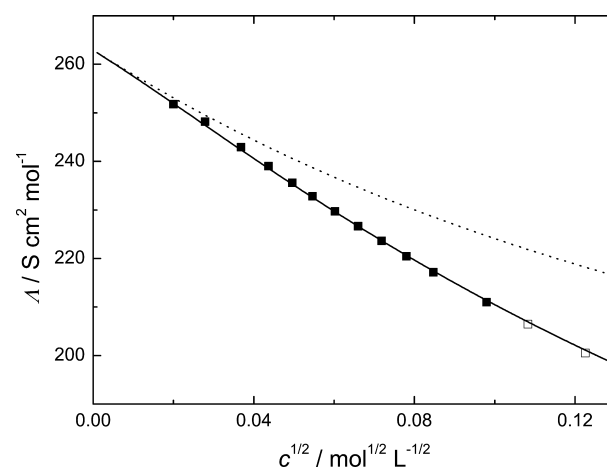


**Figure 3.** Molar conductivity,  $\Lambda_{\text{Gdm}_2\text{SO}_4}$ , of aqueous solutions of Gdm<sub>2</sub>SO<sub>4</sub> at 298.15 K. Symbols represent experimental data. The models described in the text were fitted to the full symbols, and the open symbols were not taken into account, as the concentration is already slightly above the range for which eqs 2 and 4 are valid.<sup>24</sup> The dotted line represents the limiting case of a fully dissociated electrolyte, and the solid lines show our model that accounts for the formation of GdmSO<sub>4</sub><sup>−</sup> ion pairs (see text).

the molar conductivity can be expressed as the sum of the conductances of the individual ions:

$$\Lambda_{\text{GdmCl}} = \lambda_{\text{Gdm}^+} + \lambda_{\text{Cl}^-} \quad (5)$$

The molar conductivity of the cation,  $\lambda_{\text{Gdm}^+}$ , and of the anion,  $\lambda_{\text{Cl}^-}$ , were obtained using eq 2. The hydrodynamic radius of the chloride ion is assumed to be  $r_{\text{S,Cl}^-} = 181$  pm,<sup>43</sup> and we fix the radius of the Gdm<sup>+</sup> cation to  $r_{\text{S,Gdm}^+} = 250$  pm (calculated from the data of ref 19 as the average radius of the oblate spheroid). The exact values for the ionic radii are not very critical and do not bias our results significantly. The limiting ionic conductivity

**Table 3.** Molar Concentrations,  $c$ , and Measured Molar Conductivities,  $\Lambda_m$ , for Dilute Aqueous Solutions of Gdm<sub>2</sub>SO<sub>4</sub> and Gdm<sub>2</sub>CO<sub>3</sub> at 298.15 K<sup>a</sup>

Gdm <sub>2</sub> SO <sub>4</sub>				Gdm <sub>2</sub> CO <sub>3</sub>				
$c$ (mol m <sup>−3</sup> )	$\Lambda_m$ (S cm <sup>2</sup> mol <sup>−1</sup> )	$\Lambda_c$ (S cm <sup>2</sup> mol <sup>−1</sup> )	$\alpha$	$c$ (mol m <sup>−3</sup> )	$\Lambda_m$ (S cm <sup>2</sup> mol <sup>−1</sup> )	$\Lambda_c$ (S cm <sup>2</sup> mol <sup>−1</sup> )	$\beta_1$	$\beta_2$
0.39829	251.77	251.94	0.994	0.31064	285.33	289.99	0.529	0.00160
0.77681	248.19	247.44	0.989	0.56803	275.52	276.28	0.426	0.00338
1.3569	242.93	242.37	0.983	0.83336	269.29	267.55	0.367	0.00526
1.9067	239.02	238.55	0.977	1.2265	261.20	258.76	0.312	0.00805
2.4588	235.62	235.30	0.972	1.8005	251.30	250.01	0.263	0.0119
2.9825	232.80	232.59	0.967	2.5442	243.57	242.06	0.224	0.0167
3.6278	229.69	229.61	0.962	3.1918	237.95	236.78	0.201	0.0206
4.3503	226.66	226.64	0.956	4.0532	231.88	231.13	0.179	0.0255
5.1585	223.64	223.67	0.950	5.0798	225.99	225.70	0.160	0.0309
6.0919	220.46	220.61	0.944	6.1676	220.81	220.94	0.145	0.0363
7.1734	217.17	217.43	0.937	7.0989	216.88	217.43	0.135	0.0406
9.5926	211.01	211.38	0.923	7.8411	214.24	214.92	0.128	0.0439
11.729	(206.44)	(206.92)	(0.912)	9.9301	207.56	208.87	0.113	0.0526
15.028	(200.53)	(201.10)	(0.898)	12.369	(201.44)	(203.11)	(0.100)	(0.0616)
				17.241	(191.70)	(194.19)	(0.0839)	(0.0774)

<sup>a</sup>The calculated conductivities  $\Lambda_c$  (according to eqs 8 and 11) include ion association and for Gdm<sub>2</sub>CO<sub>3</sub> also the carbonate hydrolysis. Also listed are the degrees of dissociation,  $\alpha$ , for Gdm<sub>2</sub>SO<sub>4</sub> (eq 7). The dissociation constants  $\beta_1$  and  $\beta_2$  correspond to the degree of dissociation of the carbonate ion (eq 9) and the degree of association for the GdmCO<sub>3</sub><sup>−</sup> ion pair (eq 10), respectively. For both calculated values, the conductance of the ion pair is neglected (see text). Values in parentheses were not used during the fitting procedure, as the concentration is already slightly above the range for which eqs 2 and 4 are valid.<sup>24</sup>



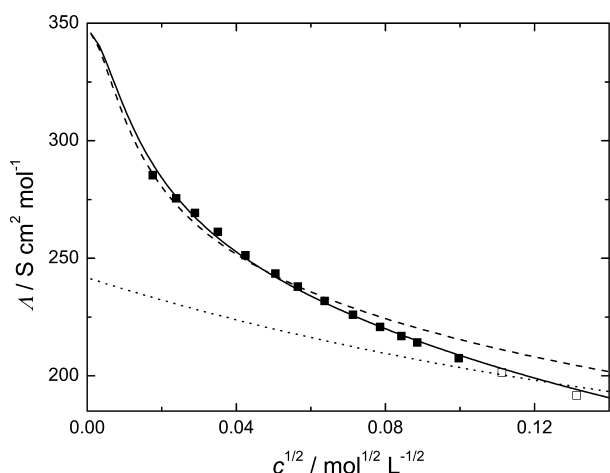


**Figure 4.** Molar conductance,  $\Lambda_{\text{Gdm}_2\text{CO}_3}$  of aqueous solutions of  $\text{Gdm}_2\text{CO}_3$  at 298.15 K. Symbols correspond to experimental data. The models described in the text were fitted to the full symbols, and the open symbols were not taken into account, as the concentration is already slightly above the range for which eqs 2 and 4 are valid.<sup>24</sup> The dotted line was obtained by assuming only  $\text{Gdm}^+$  and  $\text{CO}_3^{2-}$  to be fully dissociated in solution. The dashed line results from taking the hydrolysis of carbonate into account. The solid line is obtained including both the carbonate hydrolysis and the formation of  $\text{GdmCO}_3^-$  ion pairs (see text).

of the chloride ion has been accurately determined to  $\lambda_{\text{Cl}^-}^\circ = 76.32 \text{ S cm}^2 \text{ mol}^{-1}$ <sup>24</sup> from previous studies of other salts. Thus, the limiting molar conductivity of the guanidinium ion is the only free parameter in our model.

As can be seen in Figure 2 and Table 2, such fits are in excellent agreement with our experimental values for  $\Lambda_{\text{GdmCl}}(c)$  and we obtain the limiting ionic conductivity of the cation to be  $\lambda_{\text{Gdm}^+}^\circ = 51.54 \text{ S cm}^2 \text{ mol}^{-1}$ . The excellent agreement between the modeled conductivities, which are based on a completely dissociated electrolyte, and the experimental data indicates that  $\text{GdmCl}$  is not significantly associated in solution.

**Guanidinium Thiocyanate.** For solutions of  $\text{GdmSCN}$ , we observe a similar decrease of  $\Lambda_{\text{GdmSCN}}(c)$  as for the chloride salt. Interestingly,  $\Lambda_{\text{GdmSCN}}(c)$  virtually parallels  $\Lambda_{\text{GdmCl}}(c)$ , indicating that ion association is also negligible for aqueous solutions of  $\text{GdmSCN}$  (Figure 2). Following the data analysis for  $\text{GdmCl}$ , we model the molar conductance assuming fully dissociated ions:

$$\Lambda_{\text{GdmSCN}} = \lambda_{\text{Gdm}^+} + \lambda_{\text{SCN}^-} \quad (6)$$

The limiting molar conductivity of the thiocyanate anion is taken to be  $\lambda_{\text{SCN}^-}^\circ = 66.40 \text{ S cm}^2 \text{ mol}^{-1}$ ,<sup>24</sup> and we assume  $r_{\text{S,SCN}^-} = 213 \text{ pm}$ <sup>43</sup> for the hydrodynamic radius of the  $\text{SCN}^-$  anion. This fit, with the limiting conductivity of the guanidinium ion being the only adjustable parameter, closely follows the experimental  $\Lambda_{\text{GdmSCN}}(c)$  curve (Figure 2, Table 2). From the fit of our model to the experimental data, we extract  $\lambda_{\text{Gdm}^+}^\circ = 51.36 \text{ S cm}^2 \text{ mol}^{-1}$ , which is in good agreement with the value of  $51.54 \text{ S cm}^2 \text{ mol}^{-1}$  determined from aqueous solutions of  $\text{GdmCl}$  (see above). Analogous to the chloride salt, we find no evidence for a significant degree of aggregation of  $\text{GdmSCN}$  in solution.

**Guanidinium Sulfate.** We also study solutions of the bivalent  $\text{Gdm}_2\text{SO}_4$  salt. As will be shown below, the experimentally measured conductivities,  $\Lambda_{\text{Gdm}_2\text{SO}_4}(c)$ , are significantly lower than what would be expected for a non-associated electrolyte. We account for this apparent reduction

of the ion mobility in solution by introducing an ion association equilibrium based on single particle collisions. This means that a  $\text{Gdm}^+$  cation and a  $\text{SO}_4^{2-}$  anion form a univalent  $\text{GdmSO}_4^-$  ion pair. This association reaction is defined by its equilibrium constant  $K_{\text{GdmSO}_4^-}$  according to eq 3:

$$\begin{aligned} K_{\text{GdmSO}_4^-} &= \frac{c_{\text{GdmSO}_4^-}}{c_{\text{Gdm}^+} c_{\text{SO}_4^{2-}}} \frac{f_{\text{GdmSO}_4^-}}{f_{\text{Gdm}^+} f_{\text{SO}_4^{2-}}} \\ &= \frac{1 - \alpha}{\alpha(1 + \alpha)c} \frac{f_{\text{GdmSO}_4^-}}{f_{\text{Gdm}^+} f_{\text{SO}_4^{2-}}} \end{aligned} \quad (7)$$

To relate the equilibrium concentrations,  $c_i$ , of all species in solution to the analytical concentration of  $\text{Gdm}_2\text{SO}_4$ ,  $c$ , the degree of dissociation,  $\alpha$ , is introduced. Accordingly, the ionic strength of the solution amounts to  $I = (2\alpha + 1)c$ . To obtain  $\alpha(c)$  for a given value of  $K_{\text{GdmSO}_4^-}$ , we use eq 4 to calculate the activity coefficients  $f_i$  assuming  $r_{\text{S,Gdm}^+} = 250 \text{ pm}$ ,  $r_{\text{S,SO}_4^{2-}} = 230 \text{ pm}$ <sup>43</sup> and  $r_{\text{S,GdmSO}_4^-} = r_{\text{S,Gdm}^+} + r_{\text{S,SO}_4^{2-}} = 480 \text{ pm}$ .

Assuming these three species, i.e.,  $\text{Gdm}^+$ ,  $\text{SO}_4^{2-}$ , and  $\text{GdmSO}_4^-$ , to be present in solution, the measured conductivities,  $\Lambda_{\text{Gdm}_2\text{SO}_4}$ , can be expressed as the sum of the contributions of the individual ions:

$$\Lambda = 2\alpha\lambda_{1/2\text{SO}_4^{2-}} + (1 + \alpha)\lambda_{\text{Gdm}^+} + (1 - \alpha)\lambda_{\text{GdmSO}_4^-} \quad (8)$$

In eq 8, all single ion conductivities,  $\lambda_i(c)$ , are obtained using eq 2. To reduce the number of adjustable parameters, we take the limiting equivalent conductivity of the sulfate anion from the literature ( $\lambda_{1/2\text{SO}_4^{2-}}^\circ = 80.0 \text{ S cm}^2 \text{ mol}^{-1}$ ).<sup>25,43</sup> For the limiting molar conductivity of  $\text{Gdm}^+$ , we take  $\lambda_{\text{Gdm}^+}^\circ = 51.45 \text{ S cm}^2 \text{ mol}^{-1}$ , which is the average value determined from our studies of  $\text{GdmCl}$  and  $\text{GdmSCN}$  solutions (see above).

In Figure 3, the experimental values for  $\Lambda_{\text{Gdm}_2\text{SO}_4}(c)$  together with two different models are shown. Assuming complete dissociation of  $\text{Gdm}_2\text{SO}_4$  in solution (i.e.,  $\alpha = 1$ ,  $K_{\text{GdmSO}_4^-} = 0$  in eqs 7 and 8) yields significantly higher values for  $\Lambda_{\text{Gdm}_2\text{SO}_4}(c)$  (dotted line in Figure 3) compared to our experimental results. Such deviations give strong evidence for ion association in solution, as ion pairing leads to a reduction of the number of mobile ions in solution. We use  $K_{\text{GdmSO}_4^-}$  as an adjustable parameter in the fitting procedure to quantify this association. As we will show below, ion association is weak and the concentration of  $\text{GdmSO}_4^-$  ion pairs is rather low at all concentrations (i.e.,  $\alpha > 0.9$ , see Table 3). Thus, to reduce the number of adjustable parameters, we neglect the contribution of  $\text{GdmSO}_4^-$  to the solution conductivities to a first approximation (i.e., we neglect the last term of eq 8). Such fits yield a weak association constant of  $K_{\text{GdmSO}_4^-} = 8.6 \text{ L mol}^{-1}$  which excellently describes the measured conductivities (solid line in Figure 3, Table 3). We note that neglecting the last term of eq 8 may lead to a slight underestimation of  $K_{\text{GdmSO}_4^-}$ . However, a more realistic value for the ionic conductivity of  $\text{GdmSO}_4^-$ ,  $\lambda_{\text{GdmSO}_4^-}^\circ = 40 \text{ S cm}^2 \text{ mol}^{-1}$ ,<sup>44</sup> does not alter our results significantly and only results in a slight (30%) increase of  $K_{\text{GdmSO}_4^-}$ . Taking these uncertainties in  $\lambda_{\text{GdmSO}_4^-}^\circ$  ( $0 \leq \lambda_{\text{GdmSO}_4^-}^\circ \leq 40 \text{ S cm}^2 \text{ mol}^{-1}$ ) into account, we estimate the association constant to be in the range  $8.6 \leq K_{\text{GdmSO}_4^-} (\text{L mol}^{-1}) \leq 11.2$ .

**Guanidinium Carbonate.** As is already apparent from the raw data (Table 3),  $\Lambda_{\text{Gdm}_2\text{CO}_3}(c)$  shows a markedly different dependence on concentration than the other guanidinium salts of the present study. This is apparent from the pronounced nonlinear decrease of  $\Lambda_{\text{Gdm}_2\text{CO}_3}$  as a function of  $c^{1/2}$  (Figure 4). A second remarkable observation is the high molar conductivity at high dilutions with values for  $\Lambda_{\text{Gdm}_2\text{CO}_3}$  exceeding  $280 \text{ S cm}^2 \text{ mol}^{-1}$ . Such high conductivities cannot be explained by  $\text{Gdm}^+$  and  $\text{CO}_3^{2-}$  being solely present in solution (cf.  $2\lambda_{\text{Gdm}^+}^\circ + 2\lambda_{1/2\text{CO}_3^{2-}}^\circ \approx 240 \text{ S cm}^2 \text{ mol}^{-1}$ ).<sup>25</sup> This apparent discrepancy at high dilutions can be explained by the basicity of the carbonate ion and the accompanied formation of  $\text{OH}^-$  and  $\text{HCO}_3^-$ . The high mobility of the hydroxide ion in water leads to a significant increase of  $\Lambda_{\text{Gdm}_2\text{CO}_3}(c)$ . To model the contribution of the hydrolysis reaction to our experiments, we include the hydrolysis equilibrium in our analysis:

$$K_{\text{hyd}} = \frac{c_{\text{HCO}_3^-} c_{\text{OH}^-}}{c_{\text{CO}_3^{2-}}} \frac{f_{\text{HCO}_3^-} f_{\text{OH}^-}}{f_{\text{CO}_3^{2-}}} = \frac{c\beta_1^2}{1 - \beta_1} \frac{f_{\text{HCO}_3^-} f_{\text{OH}^-}}{f_{\text{CO}_3^{2-}}} \quad (9)$$

The activity coefficients  $f_i$  in eq 9 are obtained using eq 4 assuming the following ionic radii:  $r_{\text{S,HCO}_3^-} = 156 \text{ pm}$ ,  $r_{\text{S,CO}_3^{2-}} = 178 \text{ pm}$ , and  $r_{\text{S,OH}^-} = 133 \text{ pm}$ .<sup>43</sup> Thus, eq 9 can be used to obtain the degree of dissociation,  $\beta_1$ , at all concentrations from the analytical concentration of  $\text{Gdm}_2\text{CO}_3$ ,  $c$ , where  $K_{\text{hyd}}$  is the standard dissociation constant.

As we will show below,  $\text{Gdm}_2\text{CO}_3$  is not fully dissociated in solution and we further take the formation of ion aggregates in solution into account. Therefore, we assume the formation of  $\text{GdmCO}_3^-$  ion pairs from single particle collisions of  $\text{Gdm}^+$  and  $\text{CO}_3^{2-}$  ions. The degree of aggregation is defined by the standard association constant,  $K_{\text{GdmCO}_3^-}$ :

$$K_{\text{GdmCO}_3^-} = \frac{c_{\text{GdmCO}_3^-}}{c_{\text{Gdm}^+} c_{\text{CO}_3^{2-}}} \frac{f_{\text{GdmCO}_3^-}}{f_{\text{Gdm}^+} f_{\text{CO}_3^{2-}}} = \frac{\beta_2}{(2 - \beta_2)(1 - \beta_1 - \beta_2)c} \frac{f_{\text{GdmCO}_3^-}}{f_{\text{Gdm}^+} f_{\text{CO}_3^{2-}}} \quad (10)$$

Using activity coefficients  $f_i$  based on the ionic radii  $r_{\text{S,Gdm}^+} = 250 \text{ pm}$ ,  $r_{\text{S,CO}_3^{2-}} = 178 \text{ pm}$ , and  $r_{\text{S,GdmCO}_3^-} = 428 \text{ pm}$ , eq 10 gives the degree of association,  $\beta_2$ , at a given concentration of  $\text{Gdm}_2\text{CO}_3$ ,  $c$ . The degree of dissociation of the carbonate ion,  $\beta_1$ , in eq 10 originates from the assumption that only the  $\text{CO}_3^{2-}$  (not  $\text{HCO}_3^-$ ) can form ion aggregates. Due to the higher charge density of the carbonate (compared to hydrogencarbonate) and the resulting stronger Coulombic attraction, this assumption appears plausible. In agreement with this hypothesis, we find no significant ion association for the univalent guanidinium electrolytes  $\text{GdmCl}$  and  $\text{GdmSCN}$  that would be comparable to the hypothetical  $\text{GdmHCO}_3$ .

Both equilibria result in a reduction of the ionic strength:  $I = (3 - 2\beta_2 - \beta_1)c$ . Accordingly, the experimental  $\Lambda_{\text{Gdm}_2\text{CO}_3}$  values are related to the conductivities of the individual ions:

$$\Lambda_{\text{Gdm}_2\text{CO}_3} = (2 - \beta_2)\lambda_{\text{Gdm}^+} + 2(1 - \beta_1 - \beta_2)\lambda_{1/2\text{CO}_3^{2-}} + \beta_1(\lambda_{\text{HCO}_3^-} + \lambda_{\text{OH}^-}) + \beta_2\lambda_{\text{GdmCO}_3^-} \quad (11)$$

To obtain the ionic conductivities as a function of concentration,  $\lambda_i(c)$ , using eq 2, the limiting equivalent conductances are fixed to well established literature values:  $\lambda_{1/2\text{CO}_3^{2-}}^\circ = 69.4 \text{ S cm}^2 \text{ mol}^{-1}$ ,<sup>25</sup>  $\lambda_{\text{HCO}_3^-}^\circ = 44.5 \text{ S cm}^2 \text{ mol}^{-1}$ ,<sup>25</sup>  $\lambda_{\text{OH}^-}^\circ = 199.2 \text{ S cm}^2 \text{ mol}^{-1}$ ,<sup>25</sup> and we take  $\lambda_{\text{Gdm}^+}^\circ = 51.45 \text{ S cm}^2 \text{ mol}^{-1}$  (see above). In analogy to our model for solutions of  $\text{Gdm}_2\text{SO}_4$ , we neglect the conductance of the  $\text{GdmCO}_3^-$  ion pair to a first approximation (i.e., we neglect the last term in eq 11). Using this approach,  $K_{\text{hyd}}$  and  $K_{\text{GdmCO}_3^-}$  remain the adjustable parameters of our model for  $\Lambda_{\text{Gdm}_2\text{CO}_3}$ .

As can be seen from Figure 4, both equilibria (eqs 9 and 10) have to be taken into account to model the experimental conductivities. Neglecting both the hydrolysis of the carbonate ion and the formation of  $\text{GdmCO}_3^-$  ion pairs (i.e.,  $\beta_1 = 0$  and  $\beta_2 = 0$ ) cannot reproduce the experimental values of  $\Lambda_{\text{Gdm}_2\text{CO}_3}$  (dotted line in Figure 4). Inclusion of the hydrolysis of  $\text{CO}_3^{2-}$  and the concomitant formation of  $\text{HCO}_3^-$  and  $\text{OH}^-$  significantly improves the agreement between experiment and model at high dilutions; however, the model markedly deviates at high concentration (dashed line in Figure 4). This indicates that both the carbonate hydrolysis and ion association cannot be neglected in aqueous solutions of  $\text{Gdm}_2\text{CO}_3$ . Taking both equilibria into account, our model excellently reproduces the experimental values for  $\Lambda_{\text{Gdm}_2\text{CO}_3}(c)$  (solid line in Figure 4, Table 3).

From the fit of the above model to the experimental data, we obtain  $K_{\text{hyd}} = 2.0 \times 10^{-4} \text{ mol L}^{-1}$ . The hydrolysis constant,  $K_{\text{hyd}}$ , can also be directly calculated from the second dissociation constant of carbonic acid ( $K_{2,\text{H}_2\text{CO}_3} = c_{\text{H}^+} c_{\text{CO}_3^{2-}} / c_{\text{HCO}_3^-} = 4.603 \times 10^{-11} \text{ mol L}^{-1}$ )<sup>45</sup> and the dissociation equilibrium of water ( $K_{\text{W}} = c_{\text{H}^+} c_{\text{OH}^-} = 1.008 \times 10^{-14} \text{ mol}^2 \text{ L}^{-2}$ )<sup>25</sup>, yielding  $K_{\text{hyd}} = K_{\text{W}} / K_{2,\text{H}_2\text{CO}_3} = 2.2 \times 10^{-4} \text{ mol L}^{-1}$ , which is in very good agreement with the value obtained from our analysis. The ion pair equilibrium is rather weak, with an association constant in the range  $6.2 \leq K_{\text{GdmCO}_3^-} (\text{L mol}^{-1}) \leq 8.2$  by assuming  $0 \leq \lambda_{\text{GdmCO}_3^-}^\circ (\text{S cm}^2 \text{ mol}^{-1}) \leq 40$ <sup>44,46</sup> (see our analysis of  $\text{Gdm}_2\text{SO}_4$ ). The weak tendency of  $\text{Gdm}^+$  and  $\text{CO}_3^{2-}$  to associate in solution is broadly consistent with our earlier dielectric relaxation spectroscopy study, which yielded  $K_{\text{GdmCO}_3^-} = 4 \text{ L mol}^{-1}$ .<sup>19</sup>

## DISCUSSION

From our measurements of aqueous solutions of  $\text{GdmCl}$  and  $\text{GdmSCN}$ , we have determined the limiting molar conductivity of the guanidinium ion to be  $\lambda_{\text{Gdm}^+}^\circ = 51.45 \pm 0.10 \text{ S cm}^2 \text{ mol}^{-1}$ . This value is more accurate than previous estimations based on rough extrapolations from concentrated guanidinium salt solutions.<sup>47</sup> In fact, our value for  $\lambda_{\text{Gdm}^+}^\circ$  is surprisingly large, as it is close to the limiting conductivity of  $\text{Na}^+$  ( $\lambda_{\text{Na}^+}^\circ = 50.1 \text{ S cm}^2 \text{ mol}^{-1}$ )<sup>25</sup>, although the crystallographic radius of  $\text{Gdm}^+$ <sup>19</sup> is approximately 3 times larger than the corresponding value for  $\text{Na}^+$ .<sup>48</sup> Thus, the Stokes (hydrodynamic) radii<sup>25</sup> of both ions,  $r_{\text{S,Gdm}^+} = 178 \text{ pm}$  and  $r_{\text{S,Na}^+} = 183 \text{ pm}$  (determined independently from  $\lambda_i^\circ$ ), are practically identical and rather different from the bare ion radii,  $r(\text{Na}^+) = 102 \text{ pm}$ <sup>43</sup> and  $r(\text{Gdm}^+) = 250 \text{ pm}$  (calculated from the data of ref 19 as the average radius of the oblate spheroid). The Stokes radius is the effective radius of the hydrated ion,<sup>48</sup> and for  $\text{Na}^+$ , it is well-known that water molecules in the first hydration shell are

tightly bound and contribute to its Stokes radius, thus  $r_s(\text{Na}^+) > r(\text{Na}^+)$ .<sup>48–50</sup> Due to the disk-like shape of  $\text{Gdm}^+$ , the observation that the Stokes radius of this ion is smaller than its average geometric ratio should not be overinterpreted. Nevertheless, this result is strong evidence that the hydration shell of  $\text{Gdm}^+$  is only weakly bound, in line with previous investigations.<sup>11,19,51,52</sup>

For both monovalent guanidinium salts,  $\text{GdmCl}$  and  $\text{GdmSCN}$ , we do not find any significant degree of ion association and the experimental values for  $\Lambda$  are excellently modeled assuming a fully dissociated electrolyte, i.e.,  $K_A = 0$ . Thus, the attractive interactions of  $\text{Gdm}^+$  with  $\text{Cl}^-$  and  $\text{SCN}^-$  are too weak to overcome thermal motions at room temperature. This result, obtained for very dilute  $\text{GdmCl(aq)}$  and  $\text{GdmSCN(aq)}$  solutions, is valid up to the saturation limit as dielectric spectroscopy, which is particularly sensitive to ion pairs,<sup>49</sup> did not detect ion pairs up to the saturation limit of  $\text{GdmCl(aq)}$ , nor did molar-volume and conductivity data of concentrated solutions provide any hints at such species.<sup>19</sup> Apparently, this is at variance with molecular dynamics simulations which find a considerable number of  $\text{Cl}^-$  ions located in the first hydration shell of the  $\text{Gdm}^+$  cation.<sup>12,16</sup> However, these simulations were performed for concentrated solutions (1–6 mol L<sup>-1</sup>) where ion–ion collisions become frequent. Since the present conductivity data, as well as the dielectric relaxation study,<sup>19</sup> show that the hydration of  $\text{Gdm}^+$  and  $\text{Cl}^-$  (and  $\text{SCN}^-$ ) is weak, i.e., ion–water interactions are roughly comparable in strength to water–water interactions, it is therefore not surprising that at high concentrations of  $\text{GdmCl}$  and  $\text{GdmSCN}$  direct cation–anion contacts become frequent but these are only short-lived. It is noteworthy that molecular dynamics simulations also find a significant portion of stacked  $\text{Gdm}^+ - \text{Gdm}^+$  homoion pairs to be formed.<sup>12,53–55</sup> Although our conductivity measurements are not very sensitive to such homoion pairs as the effect of the increased hydrodynamic radius of such a species on its mobility would probably be largely compensated by the higher charge, we think that their lifetime is also short.

Unlike our results for the monovalent guanidinium salts, we find for both bivalent salts,  $\text{Gdm}_2\text{SO}_4$  and  $\text{Gdm}_2\text{CO}_3$ , a weak tendency to form ion aggregates and we relate this to the formation of ion pairs. From our modeling of the experimental values of  $\Lambda(c)$ , we obtain ion pair stability constants in the ranges  $8.6 \leq K_{\text{GdmSO}_4^-} \text{ (L mol}^{-1}\text{)} \leq 11.2$  and  $6.2 \leq K_{\text{GdmCO}_3^-} \text{ (L mol}^{-1}\text{)} \leq 8.2$ , for  $\text{GdmSO}_4^-$  and  $\text{GdmCO}_3^-$ , respectively, which is in broad accordance with earlier studies.<sup>19,56</sup> Both values are rather similar to those reported for the corresponding sodium salts, which are  $K_{\text{NaCO}_3^-} \approx 10 \text{ L mol}^{-1}$ <sup>57,58</sup> and  $K_{\text{NaSO}_4^-} \approx 7 \text{ L mol}^{-1}$ .<sup>59,60</sup> This is probably a consequence of the similar effective radii of the hydrated  $\text{Na}^+$  and essentially bare  $\text{Gdm}^+$  in aqueous solution, which results in similar Coulomb forces on the counterions.

The rather weak association also indicates that for the bivalent guanidinium salts specific interionic attractions are only moderate. At all measured concentrations, more than 90% of the ions are present as free (dissociated) ions (Table 3) and at least for  $\text{Gdm}_2\text{CO}_3\text{(aq)}$  this applies also at high concentrations.<sup>19</sup> This renders the presence of nanoscale ion aggregates arising from attractive ion–ion interactions, which has been suggested on the basis of molecular dynamics simulations of concentrated solutions,<sup>13,14</sup> rather unlikely. To be stable, such clusters would require a pronounced aggregation tendency already for dilute solutions. Furthermore, such

nanoscale entities are expected to result in very low ion mobilities, which is clearly not the case even for concentrated solutions.<sup>19</sup> Hence, we speculate that nanometer-scale ion aggregates, as they were inferred from computer simulations, may arise from packing effects or be an artifact of the molecular dynamics simulation. In fact, the used force fields<sup>20,21</sup> and the simulation time<sup>20</sup> are very critical parameters in the simulation of electrolytes. Only recently it has been shown that neglecting polarizability in simulations leads to unrealistic aggregation behavior for  $\text{Na}_2\text{SO}_4$ .<sup>21</sup> From the agreement of our present findings on the aggregation behavior of guanidinium salts with those obtained using dielectric relaxation spectroscopy, we conclude that an ion pair reduces the activity of a guanidinium ion, if the ion contact persists longer than  $\sim 40 \text{ ps}$ .<sup>19</sup> This criterion, together with our present values for the standard association constants, may be thus useful for validating molecular dynamics simulations and optimizing the used force fields.

In our present study, we find both the monovalent ( $\text{GdmCl}$  and  $\text{GdmSCN}$ ) and the divalent ( $\text{Gdm}_2\text{SO}_4$  and  $\text{Gdm}_2\text{CO}_3$ ) to be predominantly dissociated in an aqueous environment. The small degree of association for the bivalent salts does not lead to a significant reduction of the activity of the guanidinium ion in solution. Thus, ion association cannot explain the strongly enhanced protein denaturing activity of the monovalent guanidinium salts, compared to the protein stabilization of the bivalent guanidinium salts. This is in particular true, as the denaturing activity of  $\text{Gdm}^+$  is meant to originate from direct interaction of  $\text{Gdm}^+$  with proteins.<sup>2,3</sup> This leaves the question of what is the origin of their different biological activity, and it seems unlikely that it solely related to the  $\text{Gdm}^+$  cation. Our results suggest that a cooperative effect on the solution structure,<sup>61</sup> which makes the folded state of a protein energetically and entropically more/less favorable for protein stabilizing/denaturing agents,<sup>18,62</sup> respectively, appears to be more likely.

## ■ CONCLUDING REMARKS

We studied the conductance of aqueous solutions of guanidinium salts. We find the limiting ionic conductivity of the  $\text{Gdm}^+$  ion to be surprisingly similar to that of  $\text{Na}^+$ . This similarity shows that the hydration shell of the guanidinium ion is rather labile. For both monovalent ions,  $\text{GdmCl}$  and  $\text{GdmSCN}$ , our data provide no evidence for ion association in solution. For the bivalent salts  $\text{Gdm}_2\text{SO}_4$  and  $\text{Gdm}_2\text{CO}_3$ , only a weak tendency of the ions to aggregate is observed. From our analysis, we find the standard association constants to be small ( $K_A < 12$ ) for all studied guanidinium salts, which shows that the specific interionic interaction is weak. Furthermore, the values for  $K_A$  closely resemble the association constants of the corresponding sodium salts. The moderate degree of ion association observed in the present study renders the formation of ion aggregates as being the origin of the different activities of guanidinium salts toward protein unlikely, because the number of free  $\text{Gdm}^+$  ions is not significantly reduced in solution. Thus, our results suggest that the effect of guanidinium electrolytes on the stability of the tertiary structure of proteins is rather of indirect nature, with subtle changes in the entropy and enthalpy of the folded state of the protein.

## ■ AUTHOR INFORMATION

### Corresponding Author

\*E-mail: hunger@mpip-mainz.mpg.de.



## Notes

The authors declare no competing financial interest.

## ■ ACKNOWLEDGMENTS

The authors thank W. Kunz for providing access to laboratory facilities in Regensburg.

## ■ REFERENCES

- (1) Tanford, C. *Adv. Protein Chem.* **1970**, *24*, 1–95.
- (2) O'Brien, E. P.; Dima, R. I.; Brooks, B.; Thirumalai, D. *J. Am. Chem. Soc.* **2007**, *129*, 7346–7353.
- (3) Godawat, R.; Jamadagni, S. N.; Garde, S. *J. Phys. Chem. B* **2010**, *114*, 2246–2254.
- (4) von Hippel, P. H.; Wong, K.-Y. *J. Biol. Chem.* **1965**, *240*, 3909–3923.
- (5) Dempsey, C. E.; Mason, P. E.; Brady, J. W.; Neilson, G. W. *J. Am. Chem. Soc.* **2007**, *129*, 15895–15902.
- (6) Marcus, Y.; Hefter, G. *Chem. Rev.* **2006**, *106*, 4585.
- (7) Chan, A. A.; Pappu, R. V. *J. Phys. Chem. B* **2007**, *111*, 6469–6478.
- (8) Gebauer, D.; Völkel, A.; Cölfen, H. *Science* **2008**, *322*, 1819–1822.
- (9) Savelyev, A.; Papoian, G. A. *J. Am. Chem. Soc.* **2006**, *128*, 14506–14518.
- (10) Kolb, H. A.; Bamberg, E. *Biochim. Biophys. Acta* **1977**, *464*, 127–141.
- (11) Mason, P. E.; Neilson, G. W.; Dempsey, C. E.; Barnes, A. C.; Cruickshank, J. M. *Proc. Natl. Acad. Sci. U.S.A.* **2003**, *100*, 4557–4561.
- (12) Mason, P. E.; Neilson, G. W.; Enderby, J. E.; Saboungi, M.-L.; Dempsey, C. E.; MacKerell, A. D.; Brady, J. W. *J. Am. Chem. Soc.* **2004**, *126*, 11462–11470.
- (13) Mason, P. E.; Neilson, G. W.; Kline, S. R.; Dempsey, C. E.; Brady, J. W. *J. Phys. Chem. B* **2006**, *110*, 13477–13483.
- (14) Mason, P. E.; Dempsey, C. E.; Neilson, G. W.; Brady, J. W. *J. Phys. Chem. B* **2005**, *109*, 24185–24196.
- (15) Shukla, D.; Schneider, C. P.; Trout, B. L. *J. Am. Chem. Soc.* **2011**, *133*, 18713–18718.
- (16) Gannon, G.; Larsson, J. A.; Greer, J. C.; Thompson, D. *J. Phys. Chem. B* **2008**, *112*, 8906–8911.
- (17) Vazdar, M.; Uhlig, F.; Jungwirth, P. *J. Phys. Chem. Lett.* **2012**, *3*, 2021–2024.
- (18) Graziano, G. *Phys. Chem. Chem. Phys.* **2011**, *13*, 12008–12014.
- (19) Hunger, J.; Niedermayer, S.; Buchner, R.; Hefter, G. *J. Phys. Chem. B* **2010**, *114*, 13617–13627.
- (20) Hassan, S. A. *J. Phys. Chem. B* **2008**, *112*, 10573–10584.
- (21) Wernersson, E.; Jungwirth, P. *J. Chem. Theory Comput.* **2010**, *6*, 3233–3240.
- (22) Pegado, L.; Marsalek, O.; Jungwirth, P.; Wernersson, E. *Phys. Chem. Chem. Phys.* **2012**, *14*, 10248–10257.
- (23) Price, W. E.; Weingartner, H. *J. Phys. Chem.* **1991**, *95*, 8933 (and references cited therein).
- (24) Barthel, J. M. G.; Krienke, H.; Kunz, W. *Physical Chemistry of Electrolyte Solutions—Modern Aspects*; Springer: New York, 1998.
- (25) Robinson, R. A.; Stokes, R. H. *Electrolyte Solutions*, 2nd ed.; Butterworths: London, U.K., 1959.
- (26) Apelblat, A.; Bešter-Rogač, M.; Barthel, J.; Neueder, R. *J. Phys. Chem. B* **2006**, *110*, 8893–8906.
- (27) Bešter-Rogač, M.; Hunger, J.; Stoppa, A.; Buchner, R. *J. Chem. Eng. Data* **2010**, *55*, 1799–1803.
- (28) Bešter-Rogač, M.; Stoppa, A.; Hunger, J.; Hefter, G.; Buchner, R. *Phys. Chem. Chem. Phys.* **2011**, *13*, 17588–17598.
- (29) Bešter-Rogač, M.; Hunger, J.; Stoppa, A.; Buchner, R. *J. Chem. Eng. Data* **2011**, *56*, 1261–1267.
- (30) Quint, J.; Viallard, A. *J. Solution Chem.* **1978**, *7*, 137–153.
- (31) Quint, J.; Viallard, A. *J. Solution Chem.* **1978**, *7*, 525–531.
- (32) Quint, J.; Viallard, A. *J. Solution Chem.* **1978**, *7*, 533–548.
- (33) Barthel, J.; Wachter, R.; Gores, H. J. In *Modern Aspects of Electrochemistry*, Vol. 13; Conway, B. E., Bockris, J. O., Eds.; Plenum: New York, 1979.
- (34) Barthel, J.; Feuerlein, F.; Neueder, R.; Wachter, R. *J. Solution Chem.* **1980**, *9*, 209–219.
- (35) Stoppa, A.; Hunger, J.; Buchner, R. *J. Chem. Eng. Data* **2009**, *54*, 472–479.
- (36) Hoover, T. B. *J. Phys. Chem.* **1970**, *74*, 2667–2673.
- (37) Lide, D. R., Ed. *CRC—Handbook of Chemistry and Physics*, 85th ed.; CRC Press: Boca Raton, FL, 2004.
- (38) Owen, B. B.; Miller, R. C.; Milner, C. E.; Cogan, H. L. *J. Phys. Chem.* **1961**, *65*, 2065–2070.
- (39) Korson, L.; Drost-Hansen, W.; Millero, F. J. *J. Phys. Chem.* **1969**, *73*, 34–39.
- (40) Tsurko, E. N.; Neueder, R.; Barthel, J.; Apelblat, A. *J. Solution Chem.* **1999**, *28*, 973–999.
- (41) Apelblat, A.; Barthel, J. *Z. Naturforsch., A: Phys. Sci.* **1991**, *46*, 131–140.
- (42) Bešter-Rogač, M.; Neueder, R.; Barthel, J.; Apelblat, A. *J. Solution Chem.* **1997**, *26*, 537–550.
- (43) Marcus, Y. *Ion Properties*; Marcel Dekker: New York, 1997.
- (44) As the hydrodynamic radius of the  $\text{GdmSO}_4^-$  ion pair is approximately twice the radius of  $\text{SO}_4^{2-}$ , we estimate  $\lambda_{\text{GdmSO}_4^-}^\circ \approx 1/2\lambda_{1/2\text{SO}_4^{2-}}^\circ = 40 \text{ S cm}^2 \text{ mol}^{-1}$  assuming diffusive charge transport. For the  $\text{GdmCO}_3^-$  ion pair, we use the same value (i.e.,  $\lambda_{\text{GdmCO}_3^-}^\circ = 40 \text{ S cm}^2 \text{ mol}^{-1}$ ) as an upper limit (cf.  $\lambda_{1/2\text{CO}_3^{2-}}^\circ = 69.4 \text{ S cm}^2 \text{ mol}^{-1}$ ).
- (45) Millero, F.; Huang, F.; Graham, T.; Pierrot, D. *Geochim. Cosmochim. Acta* **2007**, *71*, 46–55.
- (46) Note that fixing the equilibrium constant for the carbonate hydrolysis to the corresponding literature value ( $K_{\text{hyd}} = K_{\text{W}}/K_{2,\text{H}_2\text{CO}_3} = 2.2 \times 10^{-4} \text{ mol L}^{-1}$ )<sup>45,25</sup> yields slightly higher ion pair stability constants, which are in the range  $8.8 \leq K_{\text{GdmCO}_3^-} (\text{L mol}^{-1}) \leq 10.9$ .
- (47) Marcus, Y. *J. Chem. Thermodyn.* **2012**, *48*, 70–74.
- (48) Pau, P. C. F.; Berg, J. O.; McMillan, W. G. *J. Phys. Chem.* **1990**, *94*, 2671–2679.
- (49) Buchner, R.; Hefter, G. *Phys. Chem. Chem. Phys.* **2009**, *11*, 8984.
- (50) Ohtaki, H.; Radnai, T. *Chem. Rev.* **1993**, *93*, 1157–1204.
- (51) van der Post, S. T.; Tielrooij, K. J.; Hunger, J.; Backus, E.; Bakker, H. J. *Faraday Discuss.* [Online early access]. DOI: 10.1039/C2FD20097J. Published Online: June 7, 2012.
- (52) Mountain, R. D.; Thirumalai, D. *J. Phys. Chem. B* **2004**, *108*, 19711–19716.
- (53) Boudon, S.; Wipff, G.; Maigret, B. *J. Phys. Chem.* **1990**, *94*, 6056–6061.
- (54) Soetens, J.; C.; Millot, C.; Chipot, C.; Jansen, G.; Ángyán, J. G.; Maigret, B. *J. Phys. Chem. B* **1997**, *101*, 10910–10917.
- (55) Vazdar, M.; Uhlig, F.; Jungwirth, P. *J. Phys. Chem. Lett.* **2012**, *3*, 2021–2024.
- (56) Kumar, A. *Fluid Phase Equilib.* **2001**, *180*, 195–204.
- (57) Capewell, S. G.; Buchner, R.; Hefter, G.; May, P. M. *Phys. Chem. Chem. Phys.* **1999**, *1*, 1933–1937.
- (58) Butler, J. N.; Huston, R. *J. Phys. Chem.* **1970**, *74*, 2976–2983.
- (59) Pokrovski, G. S.; Schott, J.; Sergeyev, A. S. *Chem. Geol.* **1995**, *124*, 253–265.
- (60) Capewell, S. G.; Hefter, G. T.; May, P. M. *Talanta* **1999**, *49*, 25–30.
- (61) Scott, J. N.; Nucci, N. V.; Vanderkooi, J. M. *J. Phys. Chem. A* **2008**, *112*, 10939–10948.
- (62) Hunger, J.; Tielrooij, K.-J.; Buchner, R.; Bonn, M.; Bakker, H. J. *J. Phys. Chem. B* **2012**, *116*, 4783–4795.